

Wake Effect and Power Production of Wind Turbine Arrays

Ismail^{1,4}, Samsul Kamal², Purnomo², Sarjiya³ & Sulaiman Tampubolon¹

¹ Mechanical Engineering Postgraduate Student, Universitas Gadjah Mada, Yogyakarta, Indonesia

² Mechanical Engineering, Universitas Gadjah Mada, Yogyakarta, Indonesia

³ Electrical Engineering, Universitas Gadjah Mada, Yogyakarta, Indonesia

⁴ Mechanical Engineering, Universitas Pancasila, Jakarta, Indonesia

Correspondence: Ismail, Jl. Laksda Adi Sucipto, Ori 2 No. 18 RT. 06 RW. 02 Papringan, Catur Tunggal, Sleman, Yogyakarta, Indonesia. Tel: 6-2813-8347-6846. E-mail: ismail2k7@gmail.com

Received: May 7, 2015

Accepted: May 25, 2015

Online Published: September 30, 2015

doi:10.5539/mas.v9n11p77

URL: <http://dx.doi.org/10.5539/mas.v9n11p77>

Abstract

This study experimentally investigated the influence of wake effect and production of mechanical power in wind tunnel of wind turbine arrays. Wind turbine arrays consist of 2 rows with 3 columns for spacing wind turbines in rows apart in the windward direction 1.77 rotor diameters and apart in the crosswind direction 8.85 rotor diameters. The wake characteristics such as profiles of time averaged velocity, turbulence intensity, centerline velocity deficit and wake radius for far wake regions in position 1, 2, and 3 were measured and analysed. The vertical and lateral profiles of velocity and turbulence intensity were studied. Concerning the results from measured data, empirical relations for the centerline velocity deficit, turbulence intensity and wake radius were proposed. Based on the experimental results, the power loss is due to the wake flow of upwind turbine approximately 20% when the downwind distance 8.85 rotor diameters. This is different with numerical result study that 11% at downwind distance is 8.85 rotor diameters. This difference results from the influence of ambient turbulence on the production of mechanical power of the wind turbine.

Keywords: wind turbine arrays, wind tunnel, wake effect, production of mechanical power

1. Introduction

Schreck et al (2008) have identified the most significant research topics about wind turbine dynamics, micro-siting and array effects needed for characterizing wind resources and wind power generation. The micro-siting and array of a wind turbine in the wind farm depends on a detailed knowledge of the development of the wake effect of a wind turbine. It is important to understand the interaction between the wake effect of a wind turbine and the atmospheric turbulence in order to predict its structural load and power performance (Magnusson et al., 1996; Thomsen and Sorensen, 1999). This downstream velocity deficit can lead to power losses in wind farms that are approximately 15-35% when compared to the same number of turbines in isolation (Spera, 2009; Barthelmie et al., 2009). Models to estimate wake effect (e.g., Jensen 1983; Katic 1986) and turbulence levels inside a wind farm (Frandsen and Thogersen 1999; Wessel and Lange 2004) are based on simplified assumptions and, in general, turbine sitting layouts are not designed to account for all the complex dynamics involved in a wind farm.

Most studies divided the wake effect into the near wake and far wake regions (Vermeer et al., 2003; Chu and Ching., 2014). The near wake region is considered to extend downwind of the rotor up to 1-3 rotor diameters. This region is characterized by the blade aerodynamics and the evolution of tip vortices (Whale et al., 2000). The far wake region (Hogstrom et al., 1988; Crespo and Hernandez, 1996) has found that the velocity distribution in the turbine wake exhibits a self-similar behaviour. The velocity deficit U_{c0} ($=U_0-U_c$) at the centerline of the turbine wake can be described by the following equation:

$$\frac{U_{c0}}{U_0} = k \left(\frac{r}{z} \right)^n \quad (1)$$

Where U_0 is undisturbed wind velocity at the hub height, U_c is the time averaged velocity at the centerline of wake flow, r is the rotor radius, z is the downwind distance from the turbine, k and n are constants. The experimental results show that these constants are in the range $1 < k < 3$, and $0.75 < n < 1.25$ (Hogstrom et al.,

1988; Vermeer et al., 2003).

Chu and Ching (2014) categorized experimental studies on turbine wake into two types: laboratory experiments and field studies of full-scale turbines. The effect of turbulence was investigated by Sicot et al (2006) on the power production used wind tunnel experiment of a horizontal axis wind turbine. They measured the power and thrust coefficients in three turbulence levels (4.4%, 9.0% and 12%). The results showed that the influence of turbulence on turbine power output is insignificant. The turbulence intensity, $I_t (=u'/u_{avg})$ is defined as the ratio of the root mean square of the velocity fluctuations, to the mean flow velocity.

Numerical results from Ismail et al (2014a) show that rectangular horizontal wind farm design with a rotor diameter 113 m, for spacing wind turbines in rows apart in the windward direction 1.77 rotor diameters and apart in the crosswind direction 8.85 rotor diameters constitutes of the most optimal result. Wind tunnel is used to investigate the influence of wake effect and power production in this study. Wind turbines and area used in this study to represent a wind farm to down-scale condition of the full-scale.

2. Description of Experiment Set-up

The experiments were carried out in an open-circuit, suction-type wind tunnel (Ismail et al, 2014b). Wind tunnel used at in Laboratory heat transfer & mass and mechanics fluid Department of Mechanical Engineering, Universitas Gadjah Mada. This wind tunnel has overall dimension with length of 7.59 m, wide 1.84 m and high 1.88 m, and also provided with the transparent wall and top at test section. Special on test section has the dimensions of long 2.44 m, wide 1.84 m and high 0.45 m.

The rotor blades of the wind turbine model used for the present study are made by machine 3-D Printing Fortus 250 MC with material ABS-M30. Airfoil used is NACA 4421. The blade dimension is from at root position to at tip as shown in Fig. 1. A small electricity generator was installed in the back of the turbine blades, which would produce electricity as driven by the rotating turbine blades. The wind turbine model used for the present study represents the most widely-used three-blade horizontal axial wind turbine (HAWT) in wind farm of scale smaller than it really is. As shown in Fig. 2, the rotor diameter of the wind turbine model was 0.2 m, the height of the turbine hub is 0.177 m above the wind tunnel floor, and the diameter of the turbine tower (circular pole) is 0.01 m. With the scale ratio of 1: 565, the test model would represent a wind turbine in a wind farm with the rotor diameter about 113 m and tower height about 100 m (Ismail et al, 2014a). Wind turbine setup in the section test is shown in Fig. 3. The wind velocity in test section wind tunnel was measured by a digital hot-wire anemometer (AM-4204, range 0.2-20.0 m/s) and recorded by a data acquisition system. The power generated by the wind turbine was a signal converter to direct current (GL 220, in the range 1 to 5 V) and recorded by a data acquisition system.

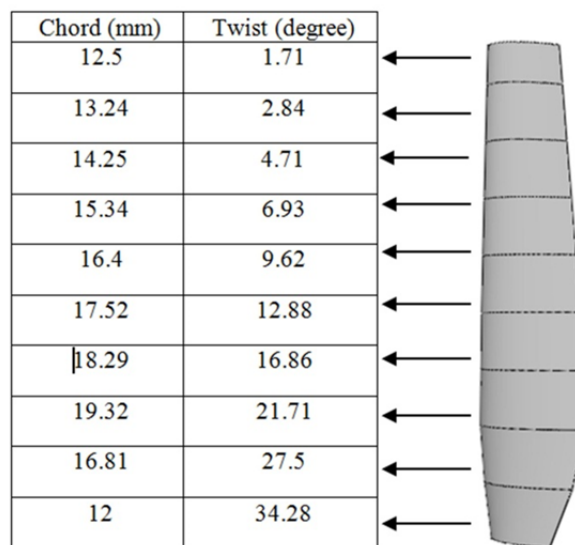


Figure 1. The blade dimension from at root position to at tip

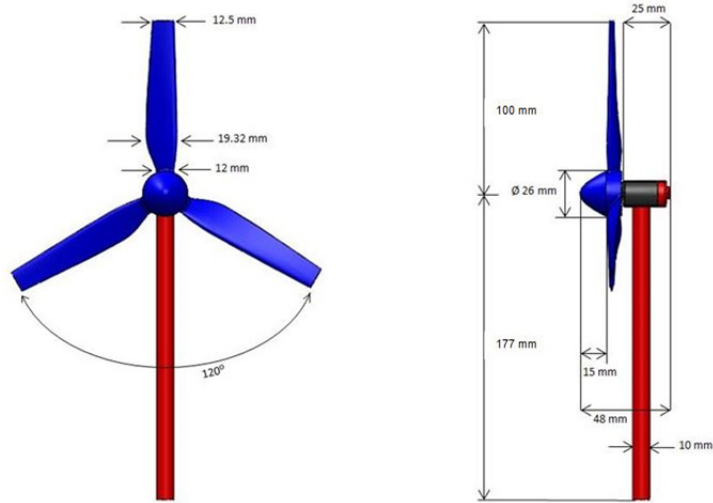
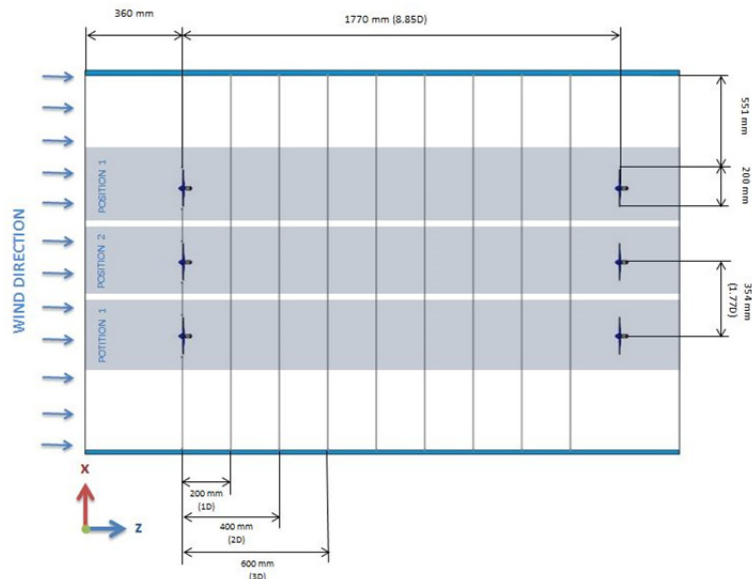
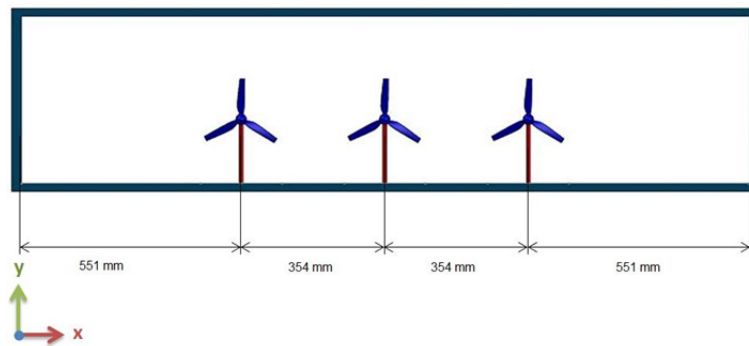


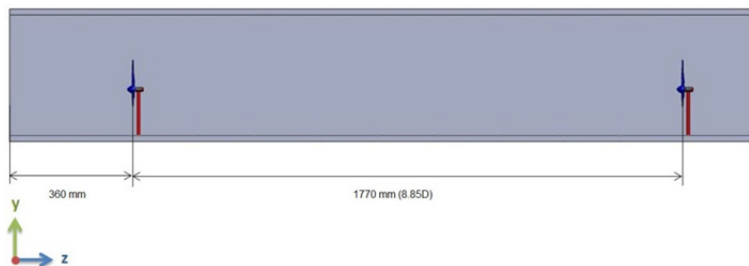
Figure 2. A schematic of the wind turbine model used in the present study



(a)



(b)

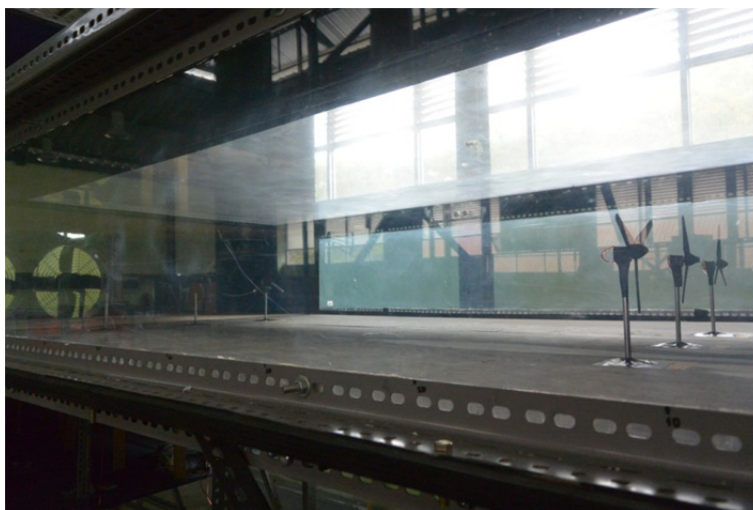


(c)

Figure 3. Schematic wind turbine setup in the section test. (a) View is upside, (b) view is in front, and (c) View is beside



(a)



(b)

Figure 4. Photograph of the experimental setup in the section test. (a) left beside, and (b) right beside

3. Results and Discussion

The results of the experiment to discuss and compares the influence of wake effect and power production. The undisturbed wind velocity $U_0 = 6.1$ m/s, 0.2 m in front of the wind turbine. It also compares vertical profiles of time averaged velocity at downwind distance $z = 1D$ up to $8D$ at position 1, 2, and 3 as shown on Fig. 5. Vertical

profiles of time averaged turbulence intensity at downwind distance $z = 1D$ up to $8D$ at position 1, 2, and 3 as shown on Fig. 6. Lateral profiles of time averaged velocity at downwind distance $z = 1D$ up to $8D$ at position 1, 2, and 3 as shown on Fig. 7. Lateral profiles of time averaged turbulence intensity at downwind distance $z = 1D$ up to $8D$ at position 1, 2, and 3 as shown on Fig. 8. The time averaged velocity $U(y)$ in the upper part of the profile is larger than the velocity in the lower part either position 1 or position 2 and 3, while the turbulence intensity $I_t(y)$ in the upper part is slightly smaller than that in the lower part. This is due to the wake flow of the turbine tower.

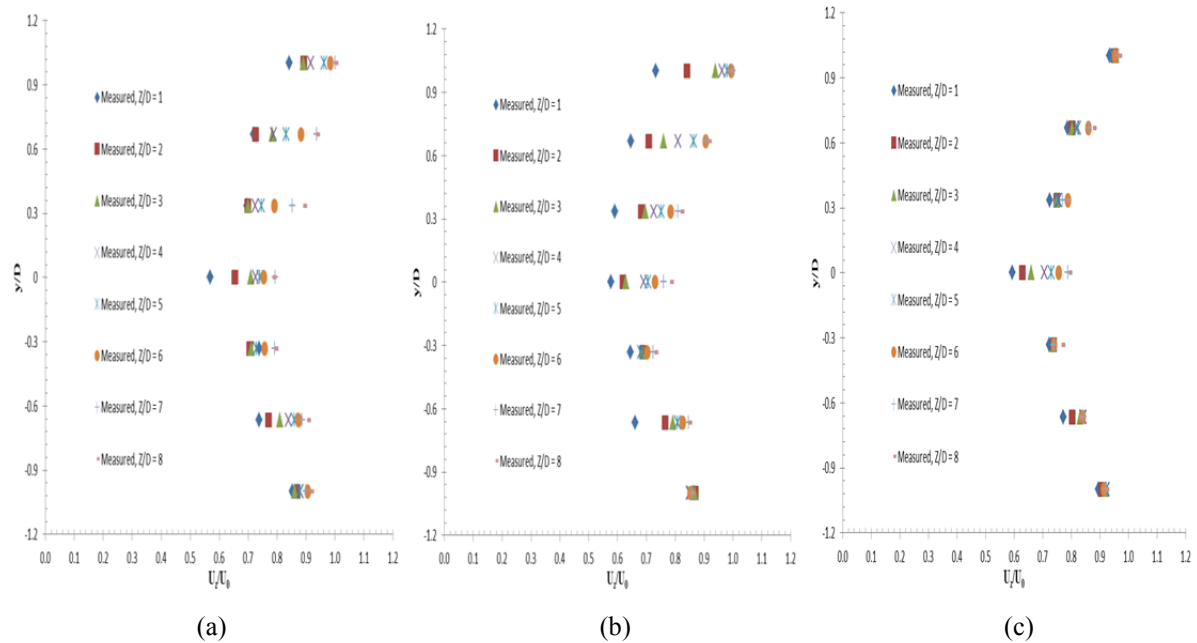


Figure 5. Vertical profiles of time averaged velocity at downwind distance $z = 1D$ up to $8D$. (a) Position 1 (b) position 2 and (c) position 3

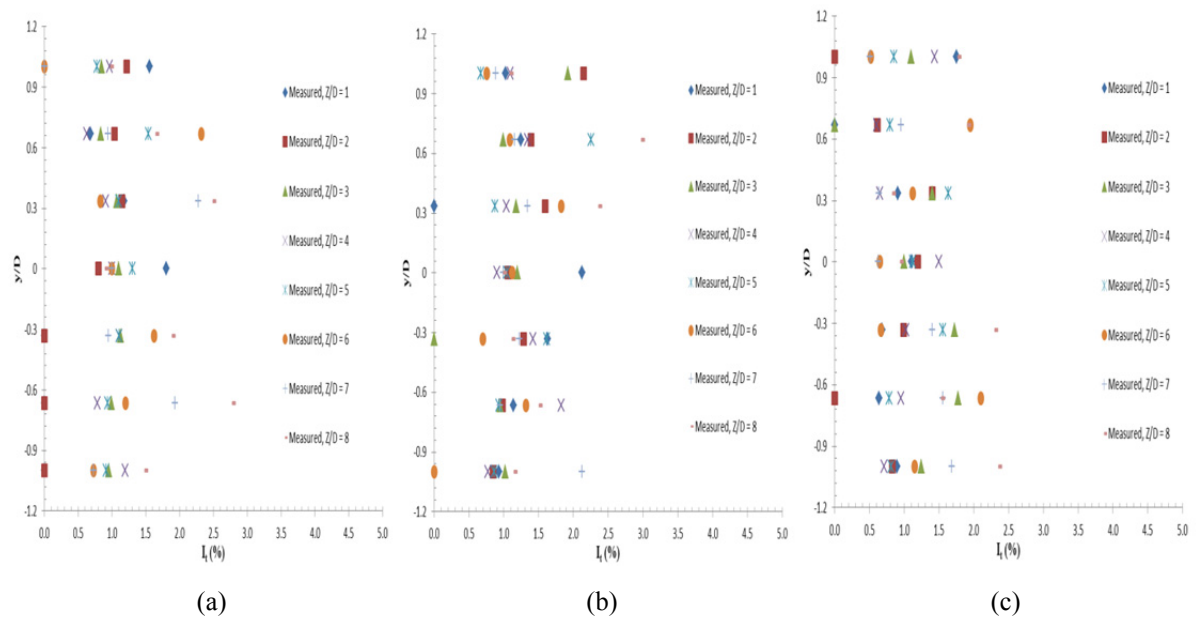


Figure 6. Vertical profiles of time averaged turbulence intensity at downwind distance $z = 1D$ up to $8D$. (a) Position 1 (b) position 2 and (c) position 3

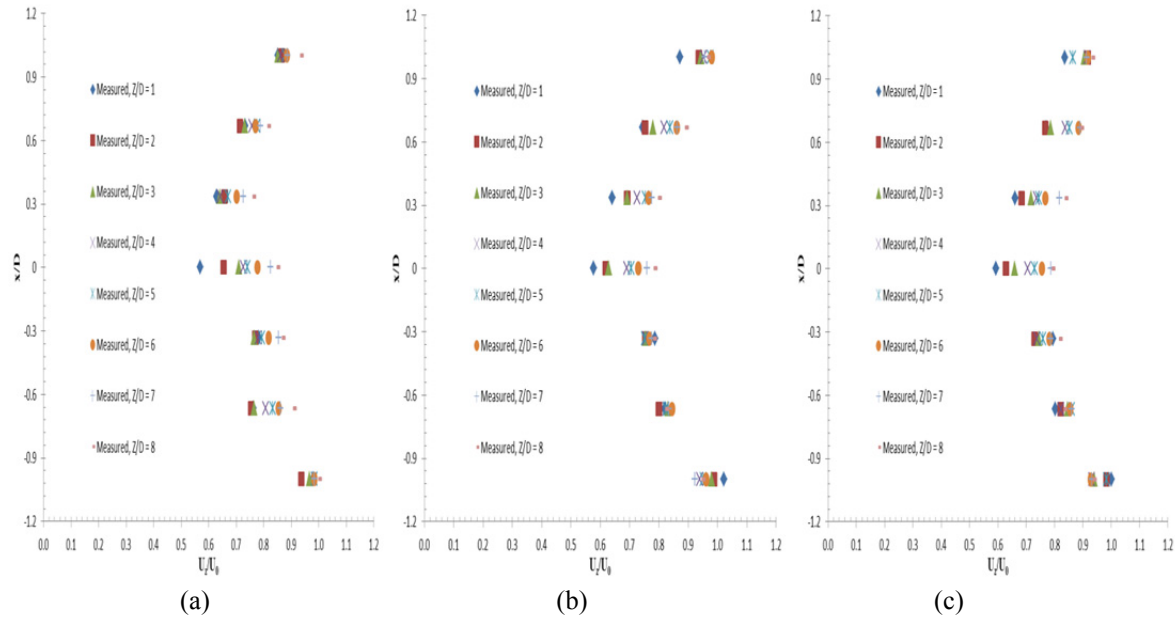


Figure 7. Lateral profiles of time averaged velocity at downwind distance $z = 1D$ up to $8D$. (a) Position 1 (b) position 2 and (c) position 3

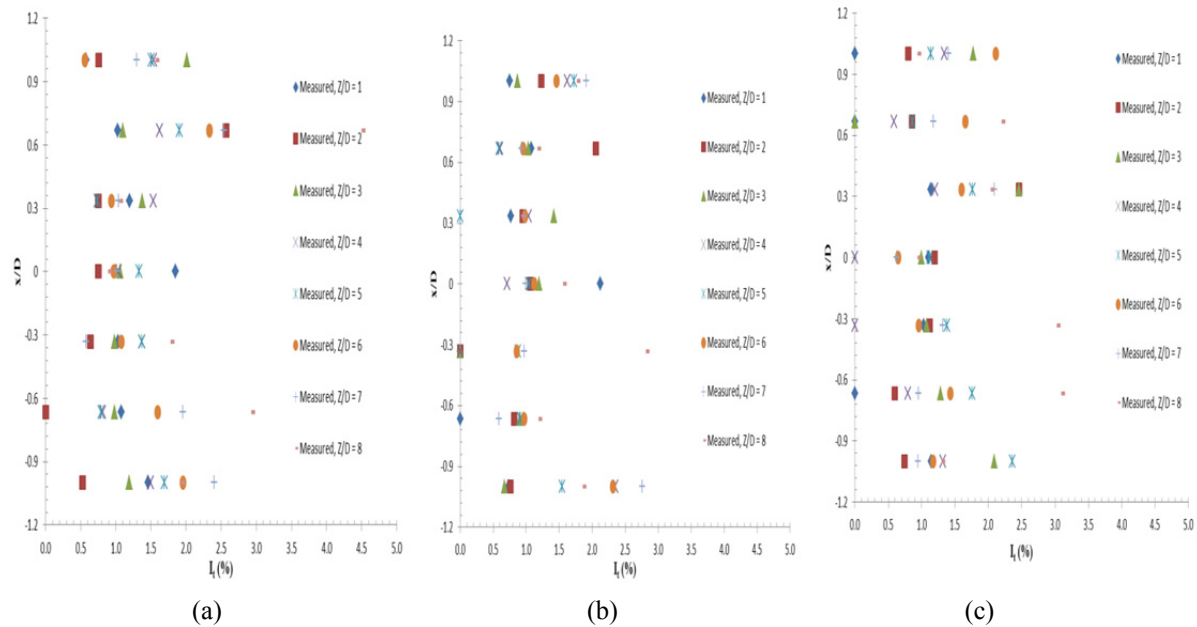


Figure 8. Lateral profiles of time averaged turbulence intensity at downwind distance $z = 1D$ up to $8D$. (a) Position 1 (b) position 2 and (c) position 3

Figure 9, 10 and 11 present the time averaged velocity profiles at different downwind distances of Position 1, 2, and 3. Because the velocity profiles are symmetrical, only the results in the positive y direction were shown. The evolutions of velocity deficit at the centerline U_{c0} at position 1, 2 and 3 are shown in Fig. 12. The values of U_{c0} decay nonlinearly as the downwind distance increases. The relationship between the centerline velocity deficit U_{c0} and the downwind distance z at position 1 can be found by using regression analysis:

$$\frac{U_{c0}}{U_0} = 0.4402 \left(\frac{r}{z}\right)^{0.352} \tag{2}$$

The coefficient of determination $R^2 = 0.8929$. In position 2, the centerline velocity deficit follows:

$$\frac{u_{co}}{u_0} = 0.6584 \left(\frac{r}{z}\right)^{0.518} \quad (3)$$

The coefficient of determination $R^2 = 0.9728$. In position 3, the centerline velocity deficit follows:

$$\frac{u_{co}}{u_0} = 0.6126 \left(\frac{r}{z}\right)^{0.524} \quad (4)$$

The coefficient of determination $R^2 = 0.9828$. Notice that the indices $n = 0.352, 0.518$ and 0.524 are smaller than the values suggested by Vermeer et al. (2003). This is because Eqs. (2), (3) and (4) such as case with Larsen et al (1996), where a turbulent wake that is diffusing with zero ambient turbulence. In position 3, the coefficient of determination $R^2 = 0.9728$ more than precision compare result position 1, $R^2 = 0.8929$ and position 2, $R^2 = 0.9728$.

Chu and Ching (2014) defined the wake radius b as the distance from the centerline to the location where the velocity $u(r) = 0.99u_0$. The wake radius as a function of downwind distances showed Fig. 13 at position 1, 2 and 3. An empirical equation for the wake radius in position 1 can be found:

$$\frac{b}{D} = 0.0171 \left(\frac{z}{D}\right) + 0.6576 \quad (5)$$

The coefficient of determination $R^2 = 0.9347$. In Position 2, the wake radius is:

$$\frac{b}{D} = 0.0289 \left(\frac{z}{D}\right) + 0.5572 \quad (6)$$

The coefficient of determination $R^2 = 0.9609$. In Position 3, the wake radius is:

$$\frac{b}{D} = 0.0269 \left(\frac{z}{D}\right) + 0.5904 \quad (7)$$

the coefficient of determination $R^2 = 0.9607$. In position 2 and 3 the wake radius almost same in the coefficient of determination and more than precision compare result in position 1.

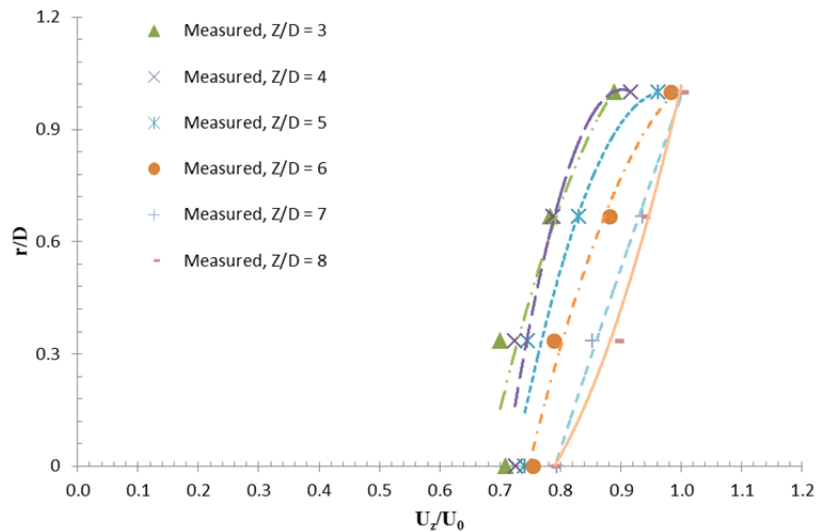


Figure 9. Time averaged velocity profiles at different downwind distances of Position 1. The symbols are the measured velocities; lines are predictions of Eq. (2)

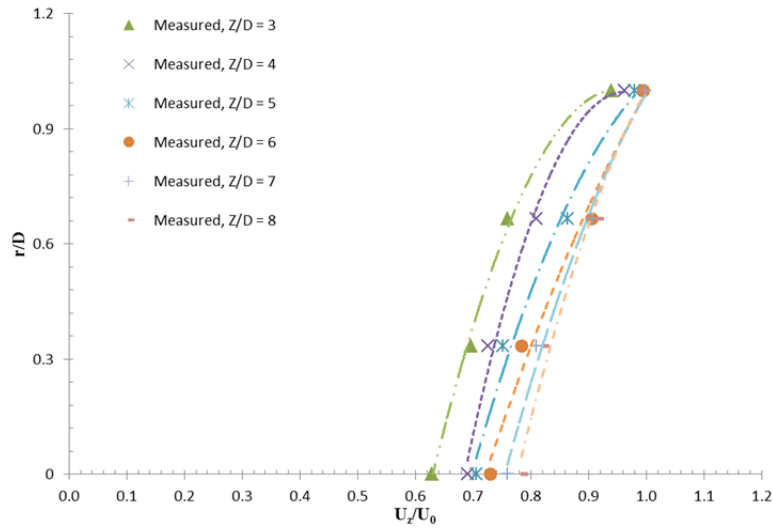


Figure 10. Time averaged velocity profiles at different downwind distances of Position 2. The symbols are the measured velocities; lines are predictions of Eq. (3)

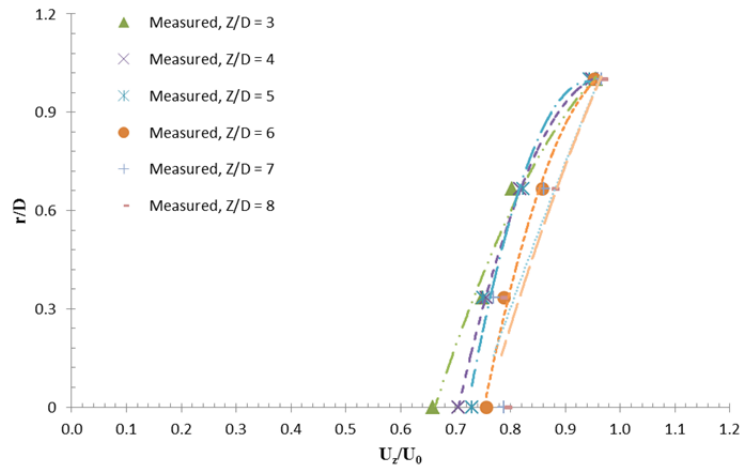


Figure 11. Time averaged velocity profiles at different downwind distances of Position 3. The symbols are the measured velocities; lines are predictions of Eq. (4).

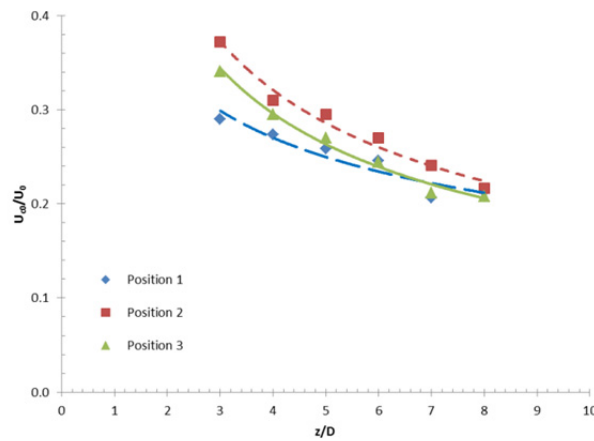


Figure 12. Centerline velocity deficit as a function of downwind distances. The symbols are the measured data; the lines are the predictions at Position 1, 2 and 3 of Eqs. (2), (3) and (4), respectively

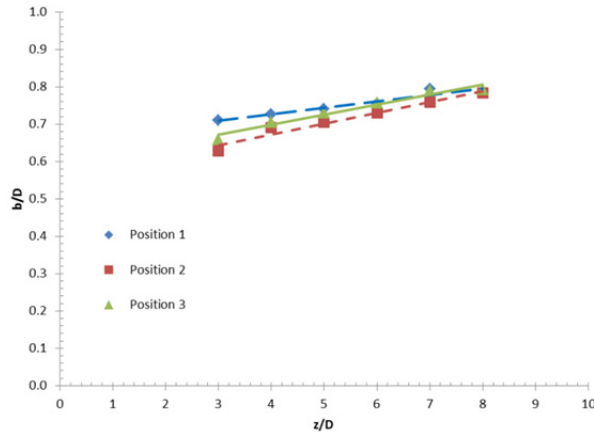


Figure 13. Wake radius as a function of downwind distances. The symbols are measured results, and the lines are the predictions at Position 1, 2 and 3 of Eqs. (5), (6) and (7), respectively

Figure 14, 15 and 16 shows turbulence intensity profiles at different downwind distances of Position 1, 2, and 3, respectively. The turbulence intensity decreased as the downwind distance increased. Fig 17 shows relationship between the centerline turbulence intensity and downwind distance. It can be described by a power law relation (Chu and Ching., 2014) :

$$I_{c0} = K \left(\frac{z}{D}\right)^{-\beta} \tag{8}$$

In position 1, coefficient $K = 1.3658$, $\beta = 0.163$. In position 2, coefficient $K = 1.2024$, $\beta = 0.089$. In position 3, coefficient $K = 2.111$, $\beta = 0.496$.

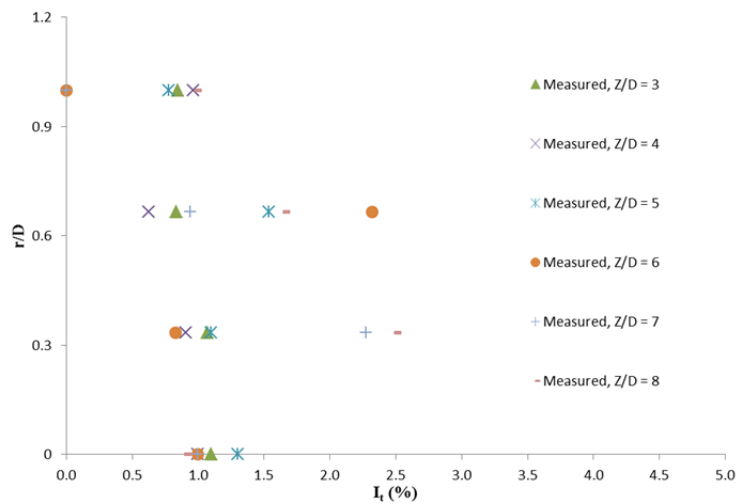


Figure 14. Turbulence intensity profiles at different downwind distances of Position 1

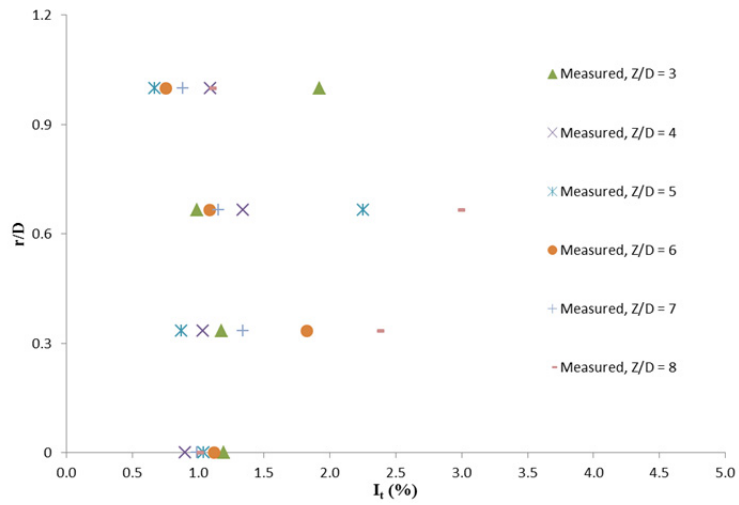


Figure 15. Turbulence intensity profiles at different downwind distances of Position 2

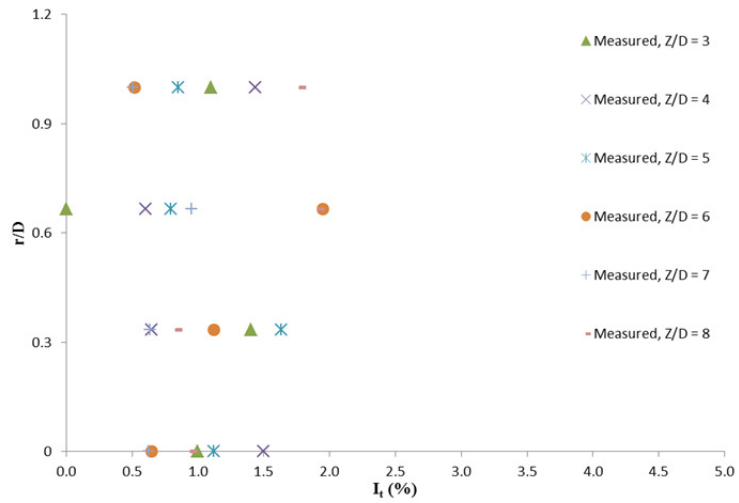


Figure 16. Turbulence intensity profiles at different downwind distances of Position 3

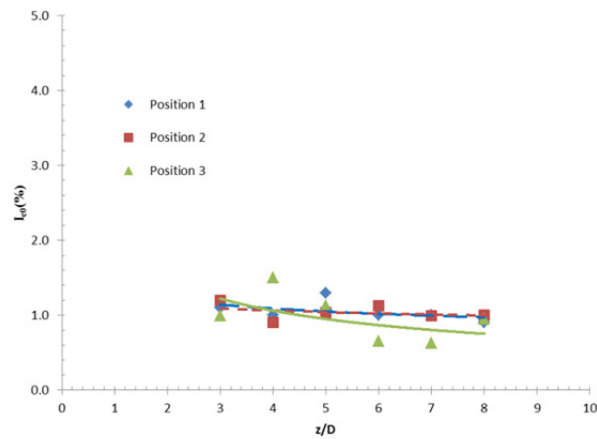


Figure 17. Centerline turbulence intensity as a function of downwind distances of Position 1,2 and 3

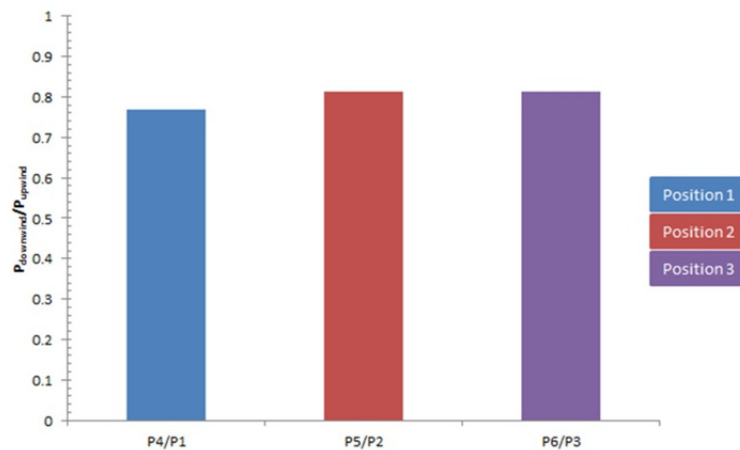


Figure 18. Compare power generated by turbine each position

In this study, the power loss is due to the velocity deficit caused by the upwind turbine, and six of horizontal axis wind turbines were installed in the test section (see Fig. 3). The production of mechanical power of upwind turbine was measured at wind speed $U_0 = 6.1$ m/s. Wind turbine arrays consist of 2 rows with 3 columns for spacing wind turbines in rows apart in the windward direction 1.77 rotor diameters and apart in the crosswind direction 8.85 rotor diameters. The distance between the centerline of the turbine to the side wall of the test section was kept at least 0.551 m ($=2.75D$) to avoid the sidewall interference. The results are shown in Fig. 18, as can be seen the generated mechanical power of downwind turbine is less than upwind turbine. The value of $P_4/P_1 = 0.77$ at position 1, $P_5/P_2 = 0.81$ at position 2, and $P_6/P_3 = 0.81$ at position 3. This result is bigger than result of study numerically from Ismail et al (2014a) show value about 0.89. This caused the influence of ambient turbulence on the production of mechanical power of the wind turbine.

4. Conclusion

This study experimentally investigated the influence of wake effect and production of mechanical power in wind tunnel of wind turbine arrays. The wake characteristics such as profiles of time averaged velocity, turbulence intensity, centerline velocity deficit and wake radius for the far wake regions in position 1, 2, and 3 were measured and analysed. The vertical and lateral profiles of velocity and turbulence intensity were studied. To the time averaged velocity and turbulence parameters of the turbine wakes were all under the influence of ambient turbulence. Concerning the results from measured data, empirical relations for the centerline velocity deficit, turbulence intensity and wake radius were proposed. This profile can be used to predict the velocity variation in terms of the centerline velocity and to validate the simulation results of the numerical models. Based on the experimental results, the power loss is due to the wake flow of upwind turbine approximately 20% when the downwind distance 8.85D. This is different with numerical result study that 11% at downwind distance 8.85D. This difference results from the influence of ambient turbulence on the production of mechanical power of the wind turbine.

Acknowledgments

The authors gratefully acknowledge the assistance of Azhim Asyratul azmi, Firman Ariyanto, Muhammad Leon Habibi and friends during of the experiment.

References

- Barthelmie, R., Frandsen, S., Hansen, K., Schepers, J., Rados, K., & Schlez, W., et al. (2009). *Modelling the impact of wakes on power output at Nysted and Horns Rev.* http://www.gl-group.com/assets/technical/301_EWEC2009presentation.pdf
- Chu, C. R., & Ching, P. H. (2014). *Turbulence effects on the wake flow and power production of a horizontal-axis wind turbine.* *J. Wind Eng. Ind. Aerodyn.* 124, 82-89. <http://dx.doi.org/10.1016/j.jweia.2013.11.001>
- Crespo, A., & Hernandez, J. (1996). *Turbulence characteristics in wind turbine wakes.* *J. Wind Eng. Ind. Aerodyn.* 61, 71-85. [http://dx.doi.org/10.1016/0167-6105\(95\)00033-X](http://dx.doi.org/10.1016/0167-6105(95)00033-X)
- Frandsen, S., & Thogersen, M. (1999). *Integrated fatigue loading for wind turbines in farms by combining ambient turbulence and wakes.* *J. Wind Eng.* 23, 327-339.

- <http://www.risoe.dk/vea/recoff/relevant/WE-final.pdf>
- Hogstrom, U., Asimakopoulus, D. N., Kambezidis, H., Helmis, C. G., & Smedman, A. (1988). *A field study of the wake behind a 2 MW wind turbine*. *Atmos. Environ*, 22(4), 803-820. [http://dx.doi.org/10.1016/0004-6981\(88\)90020-0](http://dx.doi.org/10.1016/0004-6981(88)90020-0)
- Ismail, K., Purnomo, S., & Prajitno, S. (2014a). Optimized of wind farm configuration: A case study. *Asian Journal of Applied Sciences* 02(6), 936-945. Retrieved from <http://www.ajouronline.com/index.php?journal=AJAS&page=article&op=view&path%5B%5D=2089>
- Ismail, K., Purnomo, S., & Anshary, A. A. (2014b). Design and Experiment of Open Circuit Low Speed Wind Tunnel. *Proceeding of International Conference on Green Technology*, pp. II. 30-33.
- Jensen, N. (1983). *A note on wind turbine interaction*. Riso-M-2411, Risoe National Laboratory, Roskilde, Denmark, 16 pp. Retrieved from <http://www.risoe.dk/rispubl/vea/veapdf/ris-m-2411.pdf>
- Katic, I. (1986). *A simple model for cluster efficiency*. In: *Proceedings of the European wind energy association conference and exhibition, Rome, Italy*, pp 407-409. Retrieved from <http://www.wasp.dk/~media/Sites/WASP/WASP%20support/Literature/EWEC-86paper-%20A%20Simple%20Model%20for%20Cluster%20Efficiency.ashx>
- Larsen, G. C, H^jstrup, J, & Madsen, H. A. (1996). *Wind fields in wakes*. In: Zervos A, Ehmann H, Helm P, editors. *Proceedings of the 1996 European Union Wind Energy Conference*, Goteborg, Sweden. p. 764–8.
- Magnusson, M., & Smedman, A. S. (1999). *Air flow behind wind turbines*. *J.Wind Eng. Ind. Aerodyn.*80,169–189. [http://dx.doi.org/10.1016/S0167-6105\(98\)00126-3](http://dx.doi.org/10.1016/S0167-6105(98)00126-3)
- Schreck, S., Lundquist, J., & Shaw, W. (2008). “*U. S. Department of Energy Workshop Report: Research needs for wind resource characterization*”, National Renewable Energy Laboratory Technical Report, NREL/TP-500-43521. Retrieved from <http://www.nrel.gov/docs/fy08osti/43521.pdf>
- Sicot, C., Devinant, P., Laverne, T., Loyer, S., & Hureau, J. (2006). *Experimental study of the effect of turbulence on horizontal axis wind turbine aerodynamics*. *Wind Energy*, 9(4), 361–370. <http://dx.doi.org/10.1002/we.184>
- Spera, D. (1998). *Wind turbine technology: fundamental concepts of wind turbine engineering*. New York: ASME Press. Ch. Wind Turbine Airfoils and Rotor Wakes, Lissaman, P. Retrieved from <https://www.asme.org/products/books/wind-turbine-technology-fundamental-concepts-wind>
- Thomsen, K., & Sorensen, P. (1999). *Fatigue loads for wind turbine operating in wakes*. *J. Wind Eng. Ind. Aerodyn*, 80,121–136. [http://dx.doi.org/10.1016/S0167-6105\(98\)00194-9](http://dx.doi.org/10.1016/S0167-6105(98)00194-9)
- Vermeer, L. J., Sorensen, J. N., & Crespo, A. (2003). *Wind turbine wake aerodynamics*. *Prog. Aerosp. Sci.*, 39, 467-510. [http://dx.doi.org/10.1016/S0376-0421\(03\)00078-2](http://dx.doi.org/10.1016/S0376-0421(03)00078-2)
- Whale, J., Papadopoulos, K. H., Anderson, C. G., Helmis, C. G., & Skyner, D. J. (1996). A study of the near wake structure of a wind turbine comparing measurements from laboratory and full-scale experiments. *Solar Energy*, 56(6), 621-633.
- Wessel, A., Lange, B. (2004). *A new approach for calculating the turbulence intensity inside a wind farm*. In: *Proceeding of the Deutschen Windenergiekonferenz (DEWEK)*, Wilhelmshaven.

Copyrights

Copyright for this article is retained by the author(s), with first publication rights granted to the journal.

This is an open-access article distributed under the terms and conditions of the Creative Commons Attribution license (<http://creativecommons.org/licenses/by/3.0/>).